EXPLOITATION OF STABLE HIGH-IP REGIME UNDER NEW TUNGSTEN DIVERTOR ENVIRONMENT IN KSTAR

SANG-HEE HAHN
Korea Institute of Fusion Energy (KFE)
Daejeon, Rep. of Korea
Email: hahn76@kfe.re.kr

[2]B.KIM, [1]J.W. LEE, [1]J.G. BAK, [1]J. CHUNG, [1]H. HAN, [1]Y.M. JEON, [1]J.H. JEONG, [1]M. JOUNG, [1]J.W. JUHN, [1]J. KIM, [1]J.W. KIM, [1]SUNGGUG KIM, [1]W.H. KO, [1]J.K. LEE, [1]Y.H. LEE, [1]G.W. SHIN, [1]M.H. WOO, [1]Y.U. NAM, [1]J.M. KWON
[1]Korea Institute of Fusion Energy, Daejeon, Republic of Korea
[2]UNIST, Ulsan, Republic of Korea

Abstract

The demand for high plasma current experiments in tokamak devices has been steadily increasing, driven by the need for enhanced plasma performance and relevance to ITER & DEMO; Given the stronger constraints imposed to the inductive current drive (CD) capability in the full superconducting magnet devices, various integrated control strategy development for the KSTAR plasma current ramp-up has been conducted to make the access path easier [1]. However, the installation of the W-shaped tungsten divertor at the lower side in 2023 altered the accessible density regime and thus the achievable β in KSTAR. While a detailed investigation of the effects of impurities will require further research, it is useful to determine how much the current operational space has been modified by wall material changes, through statistical analysis of the available experimental data. Preliminary statistical analysis indicates the power balance of the plasmas under the W-divertor has been modified, compared to the full-carbon divertors; the statistical distribution of plasma current(I_p), normalized current (I_p^N), used beam power, and obtained normalized beta (β_N) is examined through a collection of high I_p =0.7-1.2 MA discharges, 800 points obtained during the latest full-carbon wall era (2019-2022) and 60 points during the Tungsten divertor campaigns (2023-2024). Through the approach, it is implied that the average density increase in the W-divertor campaigns results in the relative decrease of stored energy, normalized β and increase of the required auxiliary heating power for the access of the same normalized plasma current level as the full-carbon cases.

1. INTRODUCTION

The demand for high plasma current experiments in tokamak devices has been steadily increasing each year, driven by the need for enhanced plasma performance. To maximize the triple product for fusion reactions, it is crucial to achieve the highest possible values of ion temperature, energy confinement, and plasma density. The empirically achievable plasma density maximum is directly correlated with the maximum plasma current level [1], as higher currents offer greater capacity for sustaining increased plasma density.

On the other hand, expanding the operational space of a fusion research device in terms of accessible plasma current and density will significantly benefit the physics experiments: Such shots are particularly useful in experiments that essentially require high plasma density, and are also beneficial for applications like tritium burn-up or SPI experiments, especially when the required total stored energy is higher than average values (e.g., $W_{tot} \geq 700$ kJ in KSTAR).

The shots in the high-I_p and n_e are also significantly useful for proposed parameter scans and the exploration of ITER-relevant operating regime in relatively smaller-scale devices. Such investigations are especially important for ITER because the smaller-scale superconducting magnet devices can give practical data for the realistic operation conditions, given the stronger constraints imposed to the inductive current drive (CD) capability than conventional copper devices. Inductive operation conditions in SC devices are anticipated to provide crucial information to that of ITER-relevant operations.

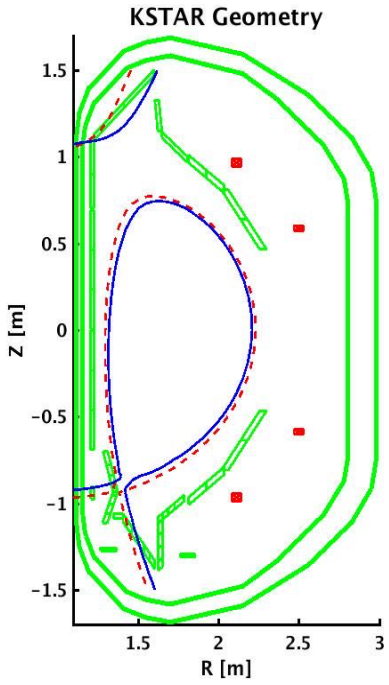

Figure 1. Comparison of boundary shape for #30280 (full carbon wall, red) and #37658 (W-divertor at lower side+ carbon walls, blue) at t=6.02s; The geometry of carbon limiters, vacuum vessel and the W-divertor is shown as green lines. The boundaries for each shot are from real-time EFIT results.

In KSTAR new integrated control strategies to control the plasma current ramp-up have been proposed and conducted, consisting of a selection of scenarios with high bootstrap, short I_p plateau, improved magnetic controls, and corresponding heating & current drive pulse design. Such integrated control allowed a series of reproducible discharges at the plasma current I_p = 0.7 ~ 1.1 MA in 2019-2022 campaigns [2]. The maximum plasma current, I_p = 1.1 MA, is sustained over 15 seconds at B_T = 2.5 T, $\delta_L \sim 0.8$, $\kappa \sim 1.8$, $\beta_N \sim 1.6$, $q_{95} \sim 3.6$, until a hardware fault stopped the pulse. Similar techniques were utilized for access of ITER-relevant high I_p plasma with matching $\beta_N \sim 2$ and shape parameters, such as $\kappa \sim 1.8$, $q_{95} \sim 3.2$; The achieved ITER-relevant pulses are distributed in two branches of I_p/B_T = 0.76-0.85 MA/1.8T, 0.9-1.1 MA/2.4-2.6T, which correspond to normalized $I_p \sim$ 0.9-1.0 [3].

With the replacement of the KSTAR lower divertor by a full tungsten configuration in late 2023 [4], changes in the design and execution of high-current experiments became inevitable. In this paper, we provide an overview of the high-current experiments conducted during the 2024 campaign, and assess the impact of the wall material change on the operational space through direct shot-by-shot comparisons as well as statistical analyses of zero-dimensional data.

2. HIGH PLASMA CURRENT ACCESS WITH W-DIVERTOR

The installation of the W-shaped Tungsten divertor at the lower side of the KSTAR vessel has brought a major change on the accessible density regime and achievable β. Such results are not unexpected, as similar trends have been observed in experiments conducted on other tokamak devices that have adopted tungsten walls, whether partial or full [3]. For example, according to the JET and ASDEX-U experiments regarding the ITER baseline (IBL) access, consistent performance decreases were reported mainly due to the increased average density; A comparison between the JET carbon wall (JET-C) and the ITER-like wall (JET-ILW) revealed a degradation in confinement, mainly indicated by H_{98y2} [5].

The ASDEX-U experiments with ITER-baseline parameters showed that the confinement factor in discharges with a full tungsten (W) wall drops to 15-20% of that with a carbon wall under the same heating conditions. The primary cause of the confinement drop is believed to be the increased Greenwald fraction. Since it is practically difficult to reduce the density sources, the AUG team suggested to introduce an alternative ITER baseline scenario operating at lower I_p and thus larger q_{95}, in order to match the ITER target $\beta_N \sim 2.0$ [6]. A cross-machine statistical study on the IBL access [7] also indicates that the effects of W impurities can make larger RMS deviation from the empirical confinement scaling IPB98(y,2), which is based mainly on the carbon-wall devices. According to the experiments from multiple machines[3], the first wall material changes into high-Z materials generally lead to reduction of confinement factor H_{98} increase of the Greenwald fraction and increase of required heating power even under same confinement. The radiation control requirements become stronger to avoid radiative collapse by high-Z impurities accumulation.

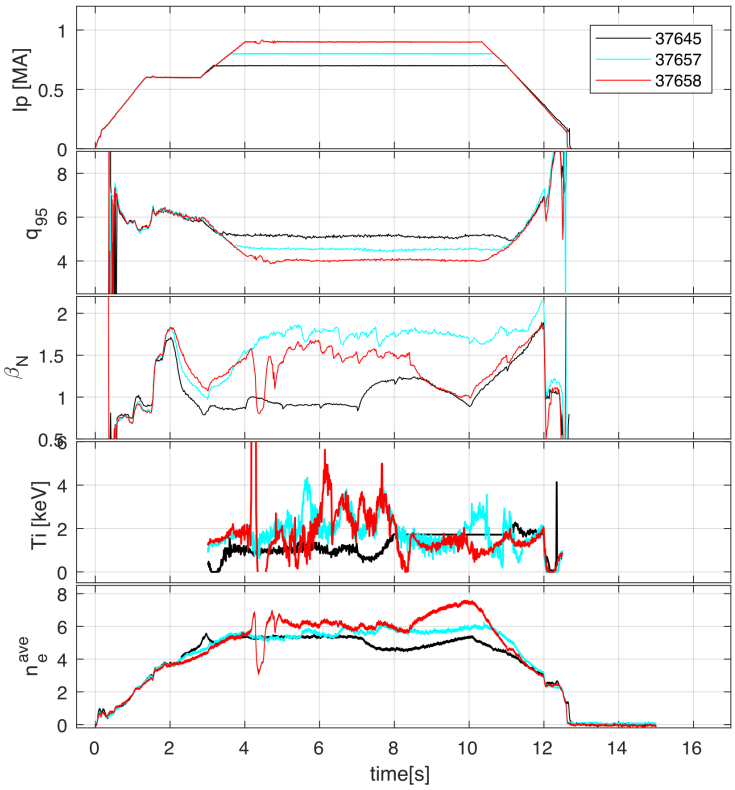

Figure 2. Three different level of I_ps with W-divertor achieved in KSTAR: I_p = 0.7, 0.8 and 0.9 MA for the shot numbers 37645, 37657 and 37658, at toroidal field B_T=2.6 Tesla. From top to bottom: plasma current (I_p [MA]), safety factor q_{95}, β_N, Ion temperature [keV] at R=2.0m, and line-averaged density in $10^{19}m^{-3}$. The heating conditions and the shape reference is the same; n_e and β_N changes at #37658, t= 8-10s are made by intentional gas puffing.

Keeping the lesson in mind, the top priorities of designing new experimental scenarios for changed wall conditions would be to minimize the impurities entering from the divertor feet when the plasma temperature is low. For the 2024 campaign scan, the best-working scenario with β_N ~1.6-2.0 was chosen: Based on the high-performance hybrid scenario developed in 2021 [8,9], a newly optimized one by incorporating different neutral beam sources, shape constraints, and radiation effects was chosen for the scan.

Pulse design follows similar criteria as the full-carbon wall cases with minor changes. Adjustments include: 1) The scenario design of new stable I_p rampup follows the same criteria as the full-carbon wall cases, and the second-I_p plateau strategy was inevitably borrowed, yet at a different I_p level. The monotonic decrease of q_{95} is also maintained while the plasma column starts at the centre (Z ~ zero) with lower elongation (κ), in order to minimize W-induced cooling before major auxiliary heating begins. 2) Various deuterium fuelling actuators, including main/divertor gas puff, pellets, and SMBI [10,11], are utilized for preventing the plasma from eating impurities, and 3) The plasma cross-section is designed to have a slightly smaller bore and lower elongation than that of the carbon wall cases, due to the divertor geometry changes. From the shape comparison in Fig. *1*, it is interesting that the triangularity does not change from the full-carbon cases, while κ decrease is inevitable for distancing from the inboard divertor surfaces. Although it is not an optimal spot for particle exhaust in the intended design, the bottom X-point was positioned to avoid unidentified particle sources from central/outboard divertor; The striking point movement in the earlier phases of the pulse was often related to unexplained disruptions.

The resulted pulse design covers a wide range of operational regime under high power conditions (P_{inj} ~ 6-8 MW). An I_p = 0.6 MA plateau prior to maximum available beam power injection is in common, and each discharge can step up to final I_p level, achieving two different operational regimes; The first regime has been achieved at I_p/B_T = 0.7MA/1.9T with $\beta_N = 2.0$, $q_{95} = 3.8$, $n_e \approx 5.5 \times 10^{19}m^{-3}$, $\beta_p = 1.2$, and stored energy W_{MHD} = 400kJ. The

second regime is performed at B_T=2.6 T, using 2-3 140 GHz gyrotrons instead, and the final I_p plateau reaches from I_p =0.8, 0.9, and 1.0MA with corresponding normalized current $I_p^N = I_p/(aB_T) \sim 0.61 - 0.76$. Figure *2* shows the key parameters of the achieved I_p=0.7, 0.8, and 0.9 MA plasmas in 2024 plasma campaign; The temporal q_{95} profile is consistent with the I_p traces, indicating the shape control was working fine. On the other hand, it was observed that the β_N (and corresponding β_p) results are more variant than the previous carbon experiments; The reason is not clear yet, which should be investigated with radiation measurements. It is also notable that the average bulk density needs to be controlled to achieve working discharge; otherwise, it was not easy to maintain the second plateau.

3. COMPARISON OF PERFORMANCES BY WALL TYPES

3.1 Direct comparison

In order to characterize the high-I_p shots obtained in these new experiments, a direct comparison was first made with plasma shots from the Carbon wall era that had similar plasma current, shape, and β_N. An example of the comparison is shown in Fig. *3*. Despite having the same plasma current target (I_p = 0.9 MA) and similar plasma shaping (See Figure *1*), the two experiments show noticeable differences in kinetic parameters, which are believed to account for the resulting differences in q_{95}. From the behavior seen at t=8-10s in #37658, it seems that the β_N is more sensitive to the density increases. It should be also noted that the ion temperature was much higher in the carbon case #30280 during the ramp-up phase – the main cause would be about 30-50% higher average density at

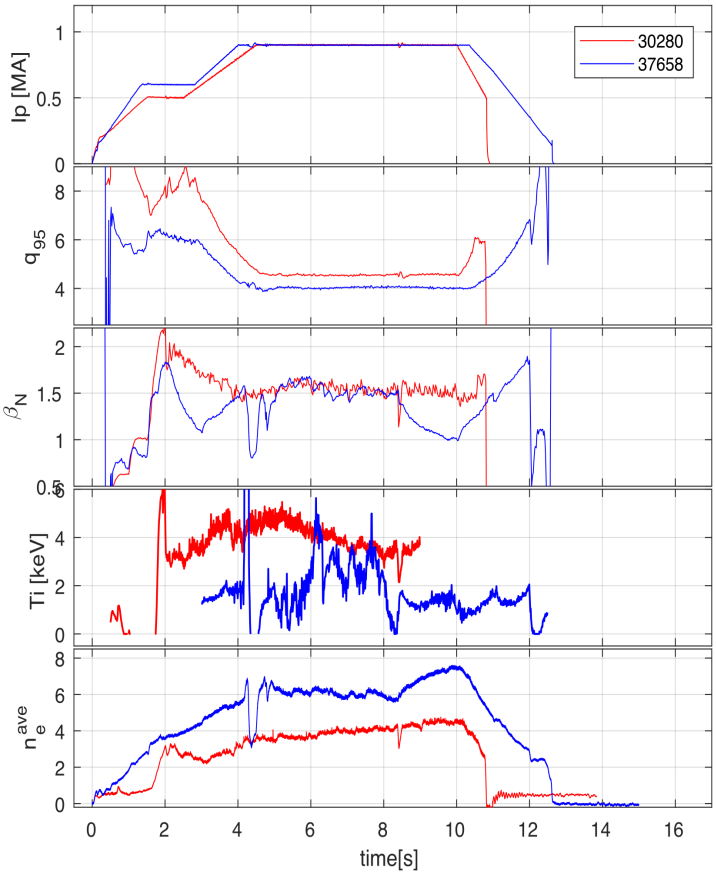

Figure 3. Direct comparison of full-carbon and W-divertor cases using shots at I_p= 0.9 MA; #30280 (carbon, red) and #37658 (W-divertor, blue); From top to bottom, plasma current (I_p [MA]), safety factor q_{95}, β_N, Ion temperature [keV] at R=2.0m, and line-averaged density in $10^{19}m^{-3}$ at B_T =2.6T. n_e and β_N changes at #37658, t= 8-10s are made by intentional gas puffing.

the same timing.

A spider chart shown in Fig. *4* indicates that the most evident difference is the bulk density, increased by approximately 30% under the tungsten wall. This increase appears to result in the rest of other parameters, especially causing reductions of both stored energy (W_{MHD}) and β_p under comparable heating conditions. Given the KSTAR geometry with minor radius $a = 0.5$ meters, the Greenwald density is calculated as $n_{GW} = 1.15 \times 10^{20}$ m^{-3}, thus the Greenwald fraction (f_{GW}) increases from 0.35 to 0.52 accordingly.

It is notable that the β_N value does not change as significantly as the drop in β_p, which may be attributed to differences in each operational scenario. Additionally, although we were not able to acquire direct measurement of the radiation by high-Z impurities, the observed decrease in core ion temperature (T_i) can imply the influence of the impurity radiation.

In fact, a shot-by-shot comparison may have limited significance, as the range of feasible early plasma ramp-up scenarios under the tungsten wall is substantially more constrained compared to the carbon wall. In several cases, scenarios involving specific X-point trajectories failed to execute properly, suggesting that the operational flexibility in plasma scenario development is narrower with the tungsten wall.

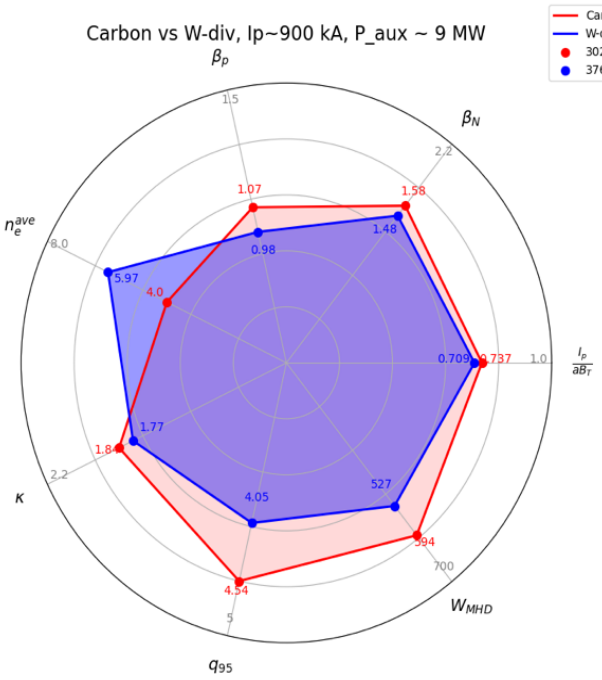

Figure 4. Spider chart to compare the full carbon (#30280, red) and the W-divertor (#37658, blue) cases; β_p, β_N, normalized current $I_N = I_p/(a * B_T)$, stored energy W_{MHD}, safety factor q_{95}, elongation κ, and line-averaged density n_e^{ave} are compared. Colored numbers indicate the value of vertices nearby.

3.2 Statistical comparison and its implications

While it would require further research in order to do a detailed investigation of the effects of impurities, which is introduced through the tungsten divertor under identical to those under the carbon wall, it would be useful to determine how much the operational space has been modified by wall material changes through statistical analysis of the available experimental data.

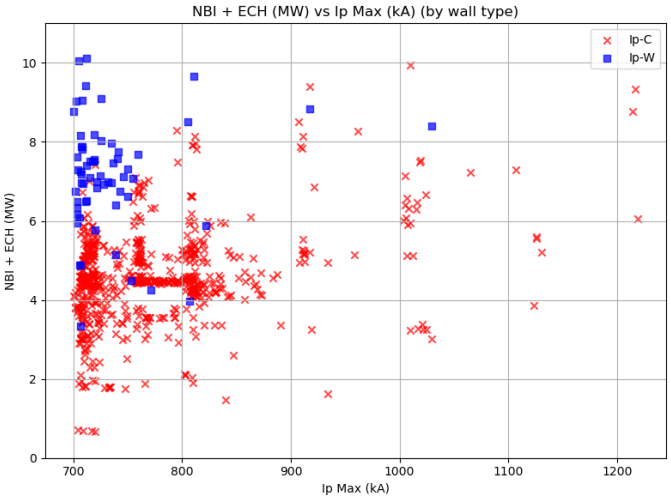

Figure 5. Scatter plot for injected total heating power [MW] and obtained plasma current I_p = 0.7 - 1.2 MA collected from 2019-2024 KSTAR campaigns; 'Ip-C' [red cross] denotes the full-carbon cases, and 'Ip-W' [blue square] the W-divertor cases.

A preliminary statistical analysis indicates the power balance of the plasmas under the W-divertor has been modified, compared to the full-carbon divertor cases; the statistical distribution of I_p, I_p^N, used beam power, and obtained β_N is examined through a collection of high I_p =0.7-1.2 MA discharges; 788 points obtained during the latest full-carbon wall campaign (2019-2022) and 63 points collected during the Tungsten divertor campaigns (2023-2024).

In this section the collected plasma data clusters are distinguished as the datapoints with the full-carbon divertor (denoted as 'Ip-C', red ×s) and the ones with the tungsten divertor (denoted as 'Ip-W', blue squares) as shown in Fig.*5-8*. The main focuses on the investigations are the relations with the heating power used for each wall clusters, which would be crucial to find further enhancement or upgrade requirements.

Figure *5* shows the achieved I_p level vs the used heating power (beam and EC gyrotrons); The first observation is that the average heating power, regardless of the heating kind, increases to obtain the same I_p under W-divertor. The vertical shift seen in the plot is about 3 MW, corresponding to approximately two beam ion source power. It is premature to determine the maximum reachable I_p yet.

On the other hand, as shown in Fig. *6*, the stored energy (W_{MHD}) obtained from the W-divertor cases completely resides within the envelope of carbon-wall cases; The implications of Figs. *5-6* are rather disappointing, to realize that the present W-divertor configuration would require more auxiliary heating power in order to obtain the plasma under the same energy level.

It is also educational to compare the dimensionless parameters with the hardware capacity (i.e. heating power). As shown in Fig. *7*, by comparing the average of each majority of data clusters, it is found that additional beam power of over 3 megawatts may be required to achieve the same level of normalized plasma current I_p^N.

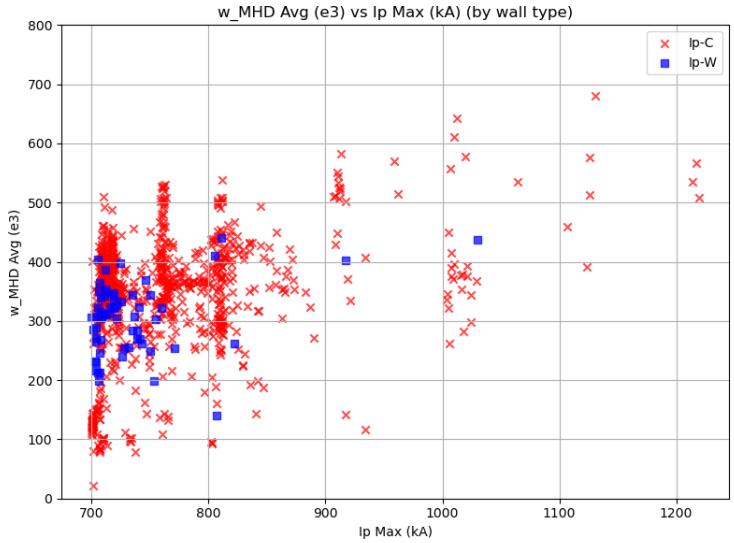

Figure 6. Scatter plot for obtained stored energy [kJ] and obtained plasma current I_p = 0.7 - 1.2 MA collected from 2019-2024 KSTAR campaigns; 'Ip-C' [red cross] denotes the full-carbon cases, and 'Ip-W' [blue square] the W-divertor cases.

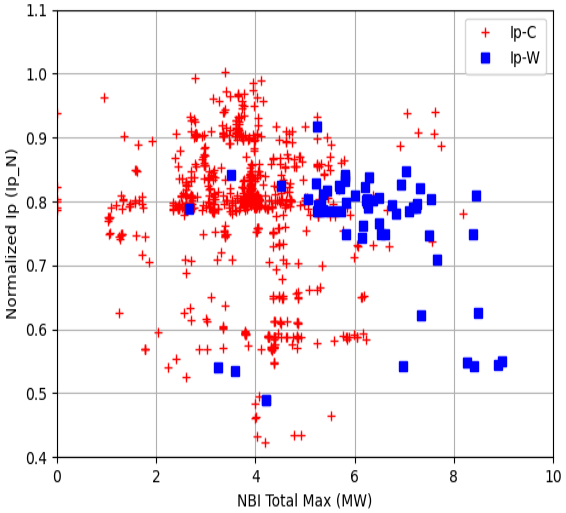

Figure 7. Scatter plot for injected beam power [MW] and obtained normalized current $I_p^N = I_p/(aB_T)$. Data points with I_p = 0.7 - 1.2 MA collected from 2019-2024 KSTAR campaigns; 'Ip-C' [red cross] denotes the full-carbon cases, and 'Ip-W' [blue square] the W-divertor cases.

The achievable normalized β under the specific wall condition can be clustered more if we control other parameters; Here the datapoints with the same normalized current (I_p^N) are used (total 530 datapoints) to see the β_N accessibility at a specific ratio of I_p/B_T. The result is shown in Fig. *8*; The segregation between the Ip-C and the Ip-W is more vivid at the total beam power maximum used.

The average β_N values for each -C and -W cluster are reported as β_N=1.91, P_{NB}=3.91 MW for the Ip-C group, and β_N = 1.63, P_{NB}=5.81 MW for the Ip-W group in Fig. *8*; it implies that an average of 1.9 MW more beam power is needed to achieve the same (β_N) under W-divertor, at I_p^N ~0.8.

These statistical observations largely match with the previously reported results from JET with a W/Be wall, and show a similar trend to ASDEX-U with a full tungsten wall, suggesting that the presence of impurities introduced through the main separatrix likely contributes to plasma performance degradation due to increased radiation. Possibilities to enhance or mitigate the tendency need to be investigated in the future experimental campaigns, especially when the planned wall upgrades target to a full tungsten wall configuration.

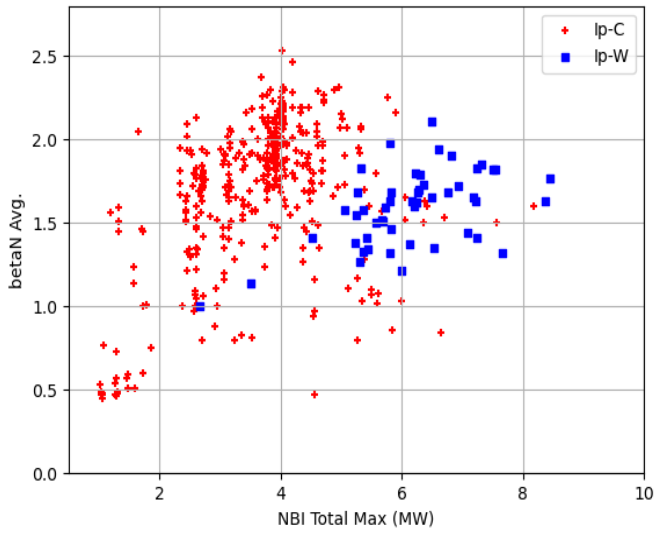

Figure 8. Scatter plot for injected beam power [MW] and obtained normalized beta β_N for the same I_p^N ~ 0.8. Total 530 data points with I_p = 0.7 - 1.2 MA are used, among the collection from 2019-2024 KSTAR campaigns; 'Ip-C' [red cross] denotes the full-carbon cases, and 'Ip-W' [blue square] the W-divertor cases.

ACKNOWLEDGEMENTS

Work supported by Korean Ministry of Science and ICT under KFE and international R&D Programs (KFE-EN2501-16, KFE-EN 2503-01, and KFE-2541-11).

REFERENCES

[1] M. Greenwald, Plasma Physics and Controlled Fusion 44 (2002) R27–R53.
[2] S.-H. Hahn, "Expansion of Stable Operating Space for High Plasma Current Toward ITER-relevant Regime in KSTAR", Proceedings in: IAEA Fusion Energy Conference, London, UK, 2023.
[3] Y.-S. Na, E. Schuster, R.V. Budny, A.M. Garofalo, S. Hahn, H.-T. Kim, et al., Nuclear Fusion 65 (2025) 093001.
[4] W.-H. Ko, S.W. Yoon, W.C. Kim, J.G. Kwak, K.L. Park, Y.U. Nam, et al., Nuclear Fusion 64 (2024) 112010.
[5] Nunes, I, the J. Contributors, Plasma Physics and Controlled Fusion 58 (2016) 014034.
[6] J. Schweinzer, M. Beurskens, L. Frassinetti, E. Joffrin, V. Bobkov, R. Dux, et al., Nuclear Fusion 56 (2016) 106007.
[7] A.C.C. Sips, J. Schweinzer, T.C. Luce, S. Wolfe, H. Urano, J. Hobirk, et al., Nuclear Fusion 58 (2018) 126010.
[8] B. Kim, M. Park, Y. Lee, S. Kim, C.-Y. Lee, S. Hong, et al., Nuclear Fusion 63 (2023) 126013.
[9] Y. Lee, S. Kim, J. Kim, B. Kim, M. Park, J. Kwon, et al., Nuclear Fusion 63 (2023) 126032.
[10] Y.O. Kim, J.I. Song, K.P. Kim, Y. Chu, K.R. Park, Fusion Engineering and Design 88 (2013) 1132–1136.
[11] G.L. Xiao, W.L. Zhong, X.R. Duan, B.B. Feng, C.Y. Chen, J. Bucalossi, et al., Reviews of Modern Plasma Physics 7 (2022).